



CLICdp-Conf-2021-001
25 May 2021

Measurement of the H to ZZ branching fraction at 350 GeV and 3 TeV CLIC

N. Vukašinović^{1a}, I. Božović-Jelisavčić^a, I. Smiljanić^a, G. Kačarević^a, G. Milutinović-Dumbelović^a, T. Agatonović-Jovin^a, M. Radulović^b, J. Stevanović^b

On behalf of the CLICdp Collaboration

^a “VINČA” Institute of Nuclear Sciences - National Institute of the Republic of Serbia, University of Belgrade, Belgrade, Serbia, ^b Faculty of Science, University of Kragujevac, Kragujevac, Serbia

Abstract

In this paper we present results of the determination of the statistical precision of the branching fraction measurement, for Higgs decaying to ZZ^* pairs at 3 TeV and 350 GeV CLIC. Measurements are simulated with the CLIC_ILD detector model, taking into consideration all relevant physics and beam-induced background processes. It is shown that the product of the branching fraction $\text{BR}(H \rightarrow ZZ^*)$ and the Higgs production cross-section can be measured with a relative statistical uncertainty of 3% (18%) at 3 TeV (350 GeV) center-of-mass energy, using semileptonic final states and assuming an integrated luminosity of 5 (1) ab^{-1} .

Talk presented at the International Workshop on Future Linear Colliders (LCWS2021), 15-18 March 2021. C21-03-15.1.

© 2021 CERN for the benefit of the CLICdp Collaboration.

Reproduction of this article or parts of it is allowed as specified in the CC-BY-4.0 license.

¹nvukasinovic@vin.bg.ac.rs

1 Introduction

The Compact Linear Collider (CLIC) is a mature option for a future Higgs factory at CERN. If approved, CLIC could be ready for construction in 2026, with the first collisions in 2035 [1]. CLIC is foreseen as a staged machine that will run at center-of-mass energies: 380 GeV¹, 1.5 TeV¹ and 3 TeV with the corresponding integrated luminosities of 1 ab⁻¹, 2.5 ab⁻¹ and 5 ab⁻¹, respectively (Figure 1 [2]).

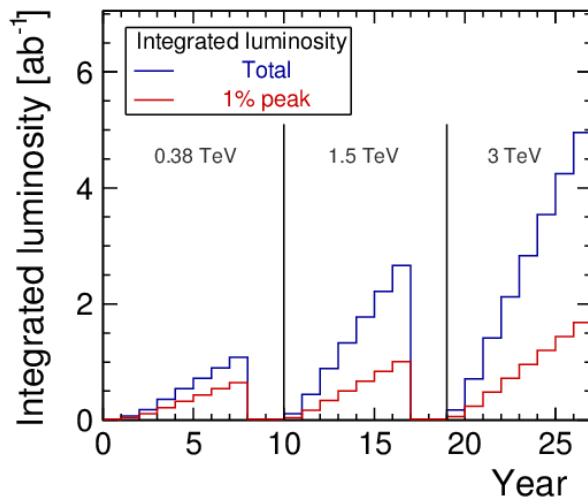


Figure 1: Luminosity per year in staged CLIC scenario. Due to the beamstrahlung the CLIC beam spectrum has a low-energy tail, so both the total luminosity per year and the luminosity collected above 99% of the nominal \sqrt{s} (labelled ‘1% peak’), are shown.

The CLIC project combines a novel two-beam acceleration scheme, with a normal-conducting modular accelerator, that has been demonstrated at the CTF3 CLIC test facility at CERN [3], along with the functionality of the main accelerator components. The drive beam is a high-current beam (about 100 A) which generates a radio-frequency field (12 GHz) that is transferred to the acceleration cavities of the main linac. In this way, conventional acceleration cavities achieve a high accelerating gradient of 100 MV/m. In the main linacs, the beam is accelerated from 190 GeV to 1.5 TeV energy. In order to maximize the reach of the CLIC physics programme, equal amounts of -80% and +80% electron beam polarisation are foreseen at the initial energy stage. At higher-energy stages, a sharing of the running time for -80% and +80% electron-beam polarisation is optimized in the ratio of 80:20 [4]. A detector for CLIC is being developed based on a broad range of full-simulation and experimental studies. In its latest model (CLICdet [5]) it comprises all-silicon vertexing and tracking components, compact Electromagnetic (ECAL) and Hadronic (HCAL) calorimeters, all placed within a magnetic field of 4 T. The excellent performance of the tracking system enables measurement of transverse momenta (p_T) with a resolution σ_{p_T}/p_T^2 of up to $2 \cdot 10^{-5} \text{ GeV}^{-1}$ for the high-energy charged particles in the central (barrel) detector region (Figure 2(a), [6]). Highly-granular calorimeters enable implementation of a Particle Flow Algorithm (PFA) [7] allowing separation of jets that originate from Higgs and vector bosons Z^0 and W^\pm . For jet energies of 50 GeV the jet energy resolution is about 5%, while for jet energies above 100 GeV jet-energy resolution is better than 3.5% as illustrated in Figure 2(b) [6]. The CLIC_ILD detector model

¹For the first CLIC energy stage at 380 GeV, additional running time devoted to a $t\bar{t}$ threshold scan near 350 GeV is foreseen. Energy of 1.5 TeV corresponds to the maximal center-of-mass energy reach with a single drive-beam complex and thus it is used in analyses as well as the initially proposed 1.4 TeV center-of-mass energy.

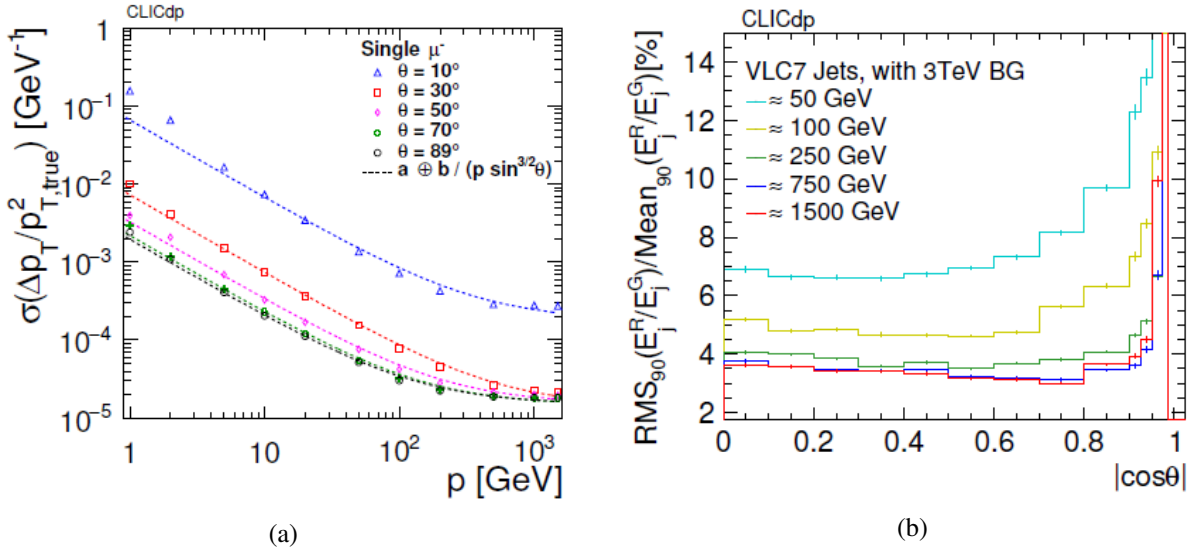


Figure 2: Transverse momentum resolution as a function of momentum for muons, at various polar angles θ (a). Jet energy resolution for different jet energies as a function of the polar angle ($|\cos\theta|$) in the presence of overlaid $\gamma\gamma \rightarrow$ hadron background. For the jet clustering, VLC algorithm [9] with a jet cone radius $R = 0.7$ (VLC7) is used (b).

[8] meets similar performances versus lepton identification efficiency and jet-energy reconstruction of relevance for this study.

2 Higgs to ZZ measurements at CLIC

Running at three different center-of-mass energies, CLIC can exploit several Higgs production mechanisms. This approach contributes to larger statistics of produced Higgs bosons, including double-Higgs production, and consequently to more precise determination of the Higgs boson properties (Higgs mass, width, couplings, etc.). At 350 (380) GeV Higgsstrahlung is the dominant Higgs production mechanism, while at higher energies WW-fusion takes over. Individual $\sigma \times \text{BR}$ measurements at all energy stages serve as input to global fits, either model-independent or model-dependent, to extract the Higgs couplings with the utmost precision. Already the fit of data to be collected in the first energy stage of CLIC operation gives better precision than HL-LHC, in particular for the Higgs couplings to c , b , W and Z (Figure 3, [10]). From Figure 3 one also reads that the Higgs to ZZ couplings can be measured with a statistical uncertainty of several permille.

3 $H \rightarrow ZZ^*$ analyses @ 350 GeV and 3 TeV

Determination of the relative statistical uncertainty of the measurements $\sigma(H\nu\bar{\nu}) \times \text{BR}(H \rightarrow ZZ^*)$ at 350 GeV and 3 TeV CLIC is done for the semileptonic $H \rightarrow ZZ^*$ final states, assuming a realistic luminosity spectrum and the presence of beamsstrahlung background. At 3 TeV, Higgs bosons are produced in WW-fusion (Figure 4(a)) with a production cross-section of 415 fb. For 5 ab^{-1} one thus expects around 6000 signal events. The signal signature at 3 TeV is $qqll$ final state and missing energy. At 350 GeV Higgs boson is produced in Higgsstrahlung process (Figure 4(b)) with a cross section of about 93.44 fb. For 1 ab^{-1} of available data one expects about 240 signal events with $qqqqll$ final state where two jets are coming from a primary Z boson decaying hadronically.

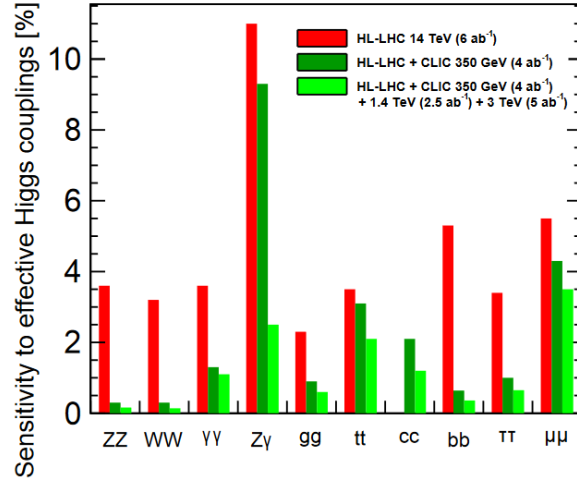


Figure 3: Projections of the model-dependent measurement of the Higgs couplings with a longer first stage CLIC, combined with the projected HL-LHC sensitivities.



Figure 4: Feynman diagrams of the dominant Higgs production mechanisms above (a) and below (b) 500 GeV center-of-mass energy.

3.1 Event selection

Since the Higgs decay products are the same in both measurements, event selections at 350 GeV and 3 TeV share common methodology. Firstly, two leptons (electrons or muons) are isolated including recovery of photons that are radiated by final state leptons (Bremsstrahlung recovery). Lepton dressing by adding photons radiated in a 3° cone improves the mass resolution of reconstructed on-shell Z bosons. The remaining particles are then grouped in 2 (4) jets by the k_T algorithm [11], where the cone radius of a jet is set to $R = 0.7$ (1.1) at 3 TeV (350 GeV) center-of-mass energy. In the preselection phase, we look for events with exactly 2 isolated leptons per event. Preselection primarily reduces backgrounds with large cross sections like $\gamma\gamma \rightarrow q\bar{q}$, $\gamma\gamma \rightarrow q\bar{q}l^+l^-$, at 3 TeV and $e^-e^+ \rightarrow q\bar{q}q\bar{q}$, $e^-e^+ \rightarrow q\bar{q}l^+l^-$, at 350 GeV. Lepton isolation is done with the Isolated Lepton Finder (ILF) Marlin processor [12] that uses several parameters in lepton isolation, including track energy of a particle (E_{track}), ratio of energy deposited in electromagnetic (ECAL) and hadronic (HCAL) calorimeters R_{CAL} ($R_{\text{CAL}} = E_{\text{ECAL}}/(E_{\text{ECAL}} + E_{\text{HCAL}})$), longitudinal z_0 , transverse d_0 , 3D impact parameter R_0 ($R_0 = \sqrt{z_0^2 + d_0^2}$) and isolation curve removing from the preselection lepton candidates with too much energy in a cone around them (E_{cone}). Figure 5 illustrates the distribution of E_{cone} versus lepton track energy (E_{track}). Since Bremsstrahlung background is more pronounced at high energy, the isolation cone contains more energy at 3 TeV than at 350 GeV and therefore loss of events with leptons on isolation curve is larger at the higher center-of-mass

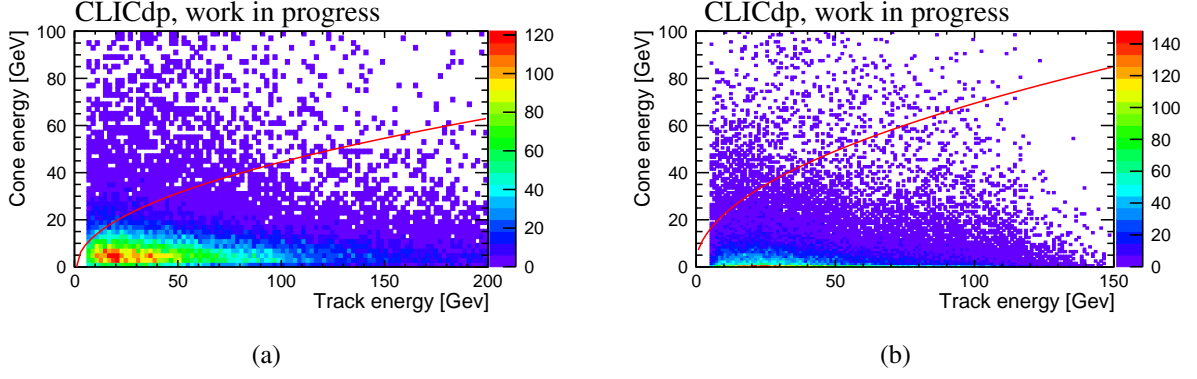


Figure 5: Cone energy as a function of track energy of the reconstructed leptons at 3 TeV (a) and at 350 GeV center-of-mass energy (b). The red line represents polynomial distribution separating isolated lepton tracks.

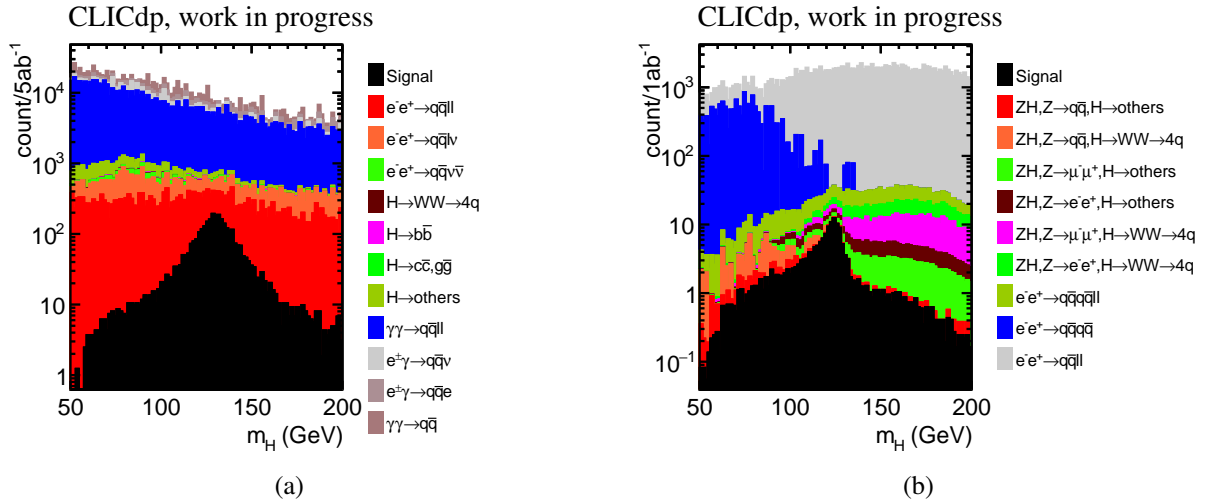


Figure 6: Stacked histograms of the Higgs invariant mass distributions after preselection phase, at 3 TeV (a) and 350 GeV (b).

energy. This effect is partially reduced with the additional requirement on minimal transverse momenta of particles in the isolation cone.

Preselection efficiencies are 67% and 77% at 3 TeV and 350 GeV, respectively. In Figure 6 (a and b), stacked histograms of the Higgs invariant mass are illustrated after the preselection phase at 3 TeV and 350 GeV, respectively.

3.2 Multivariate analysis

Final separation of signal from background is done by employing a multivariate analysis (MVA). The Toolkit for Multivariate Analysis (TMVA) [13] is applied using the Boosted Decision Tree (BDT) method in classification of events. It tends to maximize the statistical significance of signal to background separation. The statistical uncertainty δ of a measurement is derived from the statistical significance S as:

$$\delta = \frac{1}{S} = \frac{\sqrt{N_S + N_B}}{N_S} \quad (1)$$

where $N_{S(B)}$ is the number of signal (background) events. The BDT is trained on 16 (20) sensitive

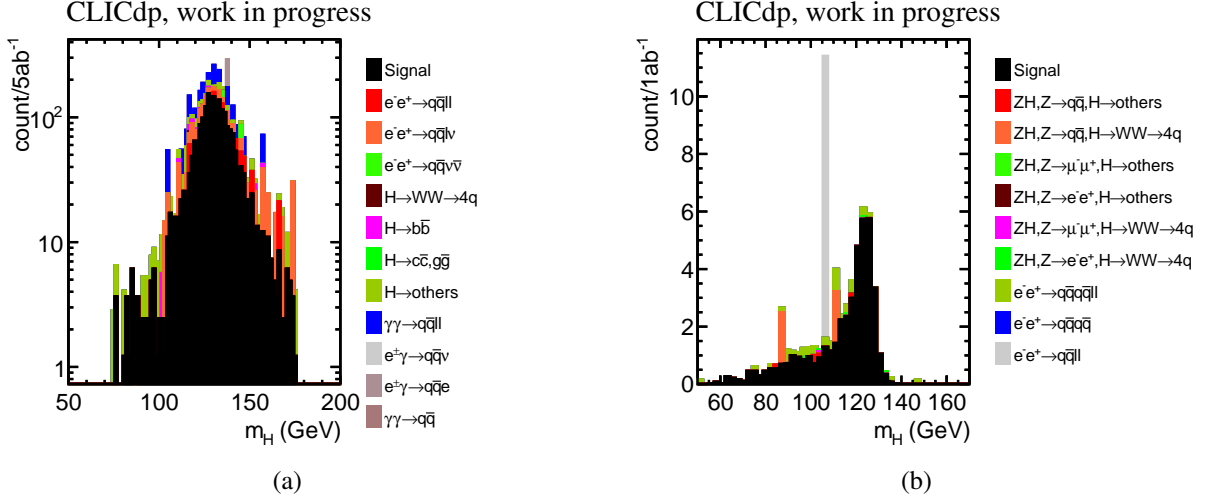


Figure 7: Stacked histograms of the Higgs invariant mass distributions after MVA, at 3 TeV (a) and 350 GeV (b) center-of-mass energies.

Table 1: Overview of the signal and the irreducible background process at 3 TeV and 350 GeV center-of-mass energies.

Process	\mathcal{E}_{presel}	\mathcal{E}_{BDT}	N_{BDT}
Signal @ 3 TeV	67%	59%	2232
Background process			
$\gamma\gamma \rightarrow q\bar{q}l^+l^-$	11‰	0.4‰	672
$e^-e^+ \rightarrow q\bar{q}lv$	3‰	6‰	509
$e^-e^+ \rightarrow Hv\bar{\nu}; H \rightarrow others$	45‰	1.6‰	328
$e^-e^+ \rightarrow q\bar{q}l^+l^-$	7.5‰	1‰	126
$e^\pm\gamma \rightarrow q\bar{q}e$	8.8‰	0.2‰	116
processes with $N_{BDT} < 100$	0.7‰	1.7‰	98
Signal @ 350 GeV			
Signal @ 350 GeV	77%	23%	43
Background process			
$e^-e^+ \rightarrow q\bar{q}l^+l^-$	11.4%	0.05‰	10
$e^-e^+ \rightarrow q\bar{q}q\bar{q}l^+l^-$	21%	5‰	5
$e^-e^+ \rightarrow HZ; Z \rightarrow q\bar{q}, H \rightarrow WW \rightarrow 4q$	0.42%	9%	4

observables at 3 TeV (350 GeV), like masses of reconstructed Z bosons, Higgs mass and polar angle, visible energy of an event, b and c-tagging probabilities of jets and jet transition variables. At both energies, the Higgs mass is most sensitive to the signal-to-background separation, that is done in a window around 126 GeV. In Figure 7 (a and b), stacked histograms of the reconstructed Higgs mass are given after MVA application, at 3 TeV (a) and 350 GeV (b) center-of-mass energies.

3.3 Statistical uncertainties

Signal BDT efficiencies are estimated to be 59% and 23%, at 3 TeV and 350 GeV, respectively. The total signal efficiency after all selection phases is 39% at 3 TeV and 18% at 350 GeV. The relatively low BDT efficiency at 350 GeV is due to the fact that the signal is very rare in nature (below 200 preselected events in 1 ab^{-1}), so the relative statistical uncertainty is sensitive even to the smallest loss of signal. Table 1 gives the expected number of selected signal and background events at 3 TeV and 350 GeV. The relative statistical uncertainty derived from statistical significance as in Eq.(1), is found to be 3% at 3 TeV and 18% at 350 GeV, assuming integrated luminosities of 5 ab^{-1} and 1 ab^{-1} , respectively. With the proposed polarization scheme of $\pm 80\%$ longitudinal electron-beam polarization and no positron polarization, the relative statistical uncertainty of the 3 TeV measurement will be conservatively decreased by a factor $\sqrt{1.48}$ [14], while the result at 350 GeV would not be relevantly influenced due to the different chiral nature of the Higgs production mechanism.

4 Conclusion

The Higgs to ZZ^* branching fraction measurement at CLIC is fully simulated at 350 GeV and 3 TeV center-of-mass energies, for the semi-leptonic final states of Higgs to ZZ^* decays. The relative statistical uncertainty of a measurement is derived from the statistical significance and is found to be 3% at 3 TeV and 18% at 350 GeV, assuming integrated luminosities 5 ab^{-1} and 1 ab^{-1} , respectively. The obtained result at 3 TeV is in line with the projection in [15].

References

- [1] Aicheler, M. et al. (eds.), *The Compact Linear Collider (CLIC) - Project Implementation Plan*, CERN, 2018, [arXiv:1903.08655](#).
- [2] Boland, M.J. et al., *Updated baseline for a staged Compact Linear Collider*, CERN, 2016 [arXiv:1608.07537](#).
- [3] Robson, A. et al., *The Compact Linear e^+e^- Collider (CLIC): Accelerator and Detector*, CERN, 2018, [arXiv:1812.07987](#).
- [4] Roloff, P. et al., *The Compact Linear e^+e^- Collider (CLIC): Physics Potential*, CLICdp-Note-2018-010, CERN, 2018.
- [5] Alipour Tehrani, N. et al. [CLICdp Collaboration], *CLICdet: The post-CDR CLIC detector model*, CLICdp-Note-2017-001, CERN, Geneva, 2017.
- [6] Arominski D. et al. [CLICdp Collaboration], *A detector for CLIC: main parameters and performance*, CERN, Geneva, 2018, [arXiv:1812.07337](#).
- [7] Thomson, M.A., *Particle Flow Calorimetry and the Pandora PFA Algorithm*, Nucl. Instr. Meth. A **611**, 25 (2009), [arXiv:0907.3577](#).
- [8] L. Linssen et al. (eds.), *Physics and Detectors at CLIC: CLIC Conceptual Design Report*, CERN-2012-003, CERN, 2012.
- [9] Boronat M. et al., *Jet reconstruction at high-energy electron-positron colliders*, Eur. Phys. J. C **78**, 144 (2018), [arXiv:1607.05039](#).
- [10] Robson, A. and Roloff, P. and de Blas, J., *CLIC Higgs coupling prospects with a longer first energy stage*, CERN, Geneva, 2020, [arXiv:2001.05278](#).

- [11] S. Catani et al., *Longitudinally-invariant k_{\perp} -clustering algorithms for hadron-hadron collisions*, Nucl. Phys. B **406**, 187 (1993).
- [12] O. Wendt, F. Gaede, T. Kramer, *Event reconstruction with MarlinReco at the ILC*, Pramana 69 (2007), [arXiv:physics/0702171](#).
- [13] A. Höcker et al., *TMVA - Toolkit for multivariate data analysis* (2009), [arXiv:physics/0703039](#).
- [14] Roloff, P. and Robson, A., *Updated CLIC luminosity staging baseline and Higgs coupling prospects*, CERN, Geneva, 2018, [arXiv:1812.01644](#).
- [15] H. Abramowicz et al. [CLICdp Collaboration], *Higgs physics at the CLIC Electron-Positron Linear Collider*, Eur. Phys. J. C 77, 475 (2017), [arXiv:1608.07538](#).